

The Diheme Cytochrome *b* Subunit (NarI) of *Escherichia coli* Nitrate Reductase A (NarGHI): Structure, Function, and Interaction with Quinolols

Richard A. Rothery¹, Francis Blasco², Axel Magalon³, and Joel H. Weiner^{1*}

¹MRC Group in the Molecular Biology of Membrane Proteins, Department of Biochemistry, 474 Medical Sciences Building, University of Alberta, Edmonton, Alberta T6G 2H7, Canada

²Laboratoire de Chimie Bactérienne, CNRS, 31 chemin Joseph Aiguier, 13402 Marseille Cedex 9, France

³Lehrstuhl für Mikrobiologie der Universität München, Maria-Ward-Strasse 1a, 80638 München, Deutschland

Abstract

Significant recent advances have been made in studies of the major dissimilatory nitrate reductase (NarGHI) of *Escherichia coli*. This enzyme is a complex iron-sulfur ([Fe-S]) molybdoenzyme that oxidizes menaquinol or ubiquinol at a periplasmically oriented Q-site (Q_P site), and reduces nitrate at a cytoplasmically-oriented molybdo-(bismolybdopterin guanine dinucleotide) (Mo-bisMGD) cofactor. The Q_P site, as well as two hemes, termed *b_L* and *b_H*, are localized in a hydrophobic diheme cytochrome *b* (NarI) that: (i) provides a conduit for electron-transfer from the periplasmically-oriented Q_P-site; (ii) provides a membrane anchoring functionality for the membrane-extrinsic subunits (NarGH) that coordinate the Mo-bisMGD (NarG) and four [Fe-S] clusters (NarH); and (iii) helps ensure the separation of sites of H⁺-yielding and H⁺-consuming reactions such that enzyme turnover leads to the generation of a proton-electrochemical potential across the cytoplasmic membrane. This minireview focuses on recent advances and future prospects for the diheme cytochrome *b* subunit (NarI) of NarGHI.

Abbreviations

DmsABC, *E. coli* DMSO reductase; *E_m*, midpoint potential; FrdABCD, *E. coli* fumarate reductase; FrdCAB, *Wolinella succinogenes* fumarate reductase; HALS, highly anisotropic low-spin; HOQNO, 2-*n*-heptyl-4-hydroxyquinoline-*N*-oxide; Mo-bisMGD, molybdo-bis(molybdopterin guanine dinucleotide); MQH₂, menaquinol; NapAB, periplasmic nitrate reductase; NarGH, membrane-extrinsic catalytic dimer; NarGHI, nitrate reductase A; NarI(ΔGH), NarI subunit in the absence of NarGH; Q-site, quinol binding site; Q_{nr}, putative Q-site located between heme *b_H* and the [3Fe-4S] cluster of NarH; Q_P site, Q-site located towards the periplasmic side of NarI; Q_P^{DMS}, proximal Q-site of *E. coli* DmsABC (proximal to the DmsAB subunits); Q_P^{FRD}, proximal quinol binding site of *E. coli* fumarate reductase (proximal to the FrdAB subunits); SdhCAB, *Bacillus subtilis* succinate dehydrogenase; TM, transmembrane segment; UQH₂, ubiquinol; Δ*E_m*, change in *E_m*.

*For correspondence. Email Joel.Weiner@UAlberta.ca; Tel. (780) 492-2761; Fax. (780) 492-0886.

Introduction

Facultative anaerobes such as *Escherichia coli* are able to grow anaerobically on nitrate by inducing a combination of two respiratory nitrate reductases (Berks *et al.*, 1995a; Moreno-Vivián *et al.*, 1999; Philippot and Højberg, 1999; Richardson and Watmough, 1999). These comprise the soluble periplasmic NapAB and the membrane-bound NarGHI (nitrate reductase A). In combination, or individually, these enzymes are able to support anaerobic growth on nitrate with a non-fermentable carbon source such as glycerol (Potter *et al.*, 1999; Potter *et al.*, 2000). A third enzyme, nitrate reductase Z (NarZYV), appears to have very similar enzymatic activity to NarGHI (Blasco *et al.*, 1990; Guigliarelli *et al.*, 1992), but is expressed at low levels and is unable to support respiratory growth (Potter *et al.*, 1999). Significant recent progress has been made in our understanding of NarGHI, enabling delineation of its prosthetic group composition and redox chemistry (Augier *et al.*, 1993a; Augier *et al.*, 1993b; Guigliarelli *et al.*, 1992; Guigliarelli *et al.*, 1996; Magalon *et al.*, 1997a; Rothery *et al.*, 1998b), as well as allowing a preliminary view of its electron-transfer pathway and catalytic mechanism (Magalon *et al.*, 1998a; Magalon *et al.*, 1997b; Rothery *et al.*, 1999a). This review focuses on the structure and function of the diheme cytochrome *b* subunit (NarI) of NarGHI which is emerging as an excellent model system for the study of membrane-intrinsic quinol-binding hemoproteins (Magalon *et al.*, 1997a; Magalon *et al.*, 1998b; Rothery *et al.*, 1999a).

NarGHI is a complex iron-sulfur molybdoenzyme comprising three subunits that coordinate a total of seven prosthetic groups (Guigliarelli *et al.*, 1992; Guigliarelli *et al.*, 1996; Rothery *et al.*, 1999a; Rothery *et al.*, 1998b). These prosthetic groups delineate an electron-transfer conduit from a site of quinol oxidation to a site of nitrate reduction. In addition, they ensure separation of the sites of proton-yielding (quinol oxidation) and proton-consuming (nitrate reduction) reactions such that enzyme turnover is coupled to the generation of a proton electrochemical potential (Berks *et al.*, 1995b; Jones *et al.*, 1980). The three subunits are: (i) a catalytic subunit (NarG, 1246 amino acid residues, 140kDa) which contains a molybdenum cofactor (molybdo-bis(molybdopterin guanine dinucleotide), Mo-bisMGD) at its active site (Magalon *et al.*, 1998a; Rothery *et al.*, 1998b); (ii) an electron-transfer subunit (NarH, 512 amino acid residues, 58kDa) which contains three [4Fe-4S] clusters and one [3Fe-4S] cluster (Augier *et al.*, 1993a; Augier *et al.*, 1993b; Guigliarelli *et al.*, 1992; Guigliarelli *et al.*, 1996; Rothery *et al.*, 1998b); and (iii) a membrane anchor subunit (NarI, 225 amino acid residues, 26kDa) which contains two hemes *b* (*b_H* and *b_L*) (Berks *et*

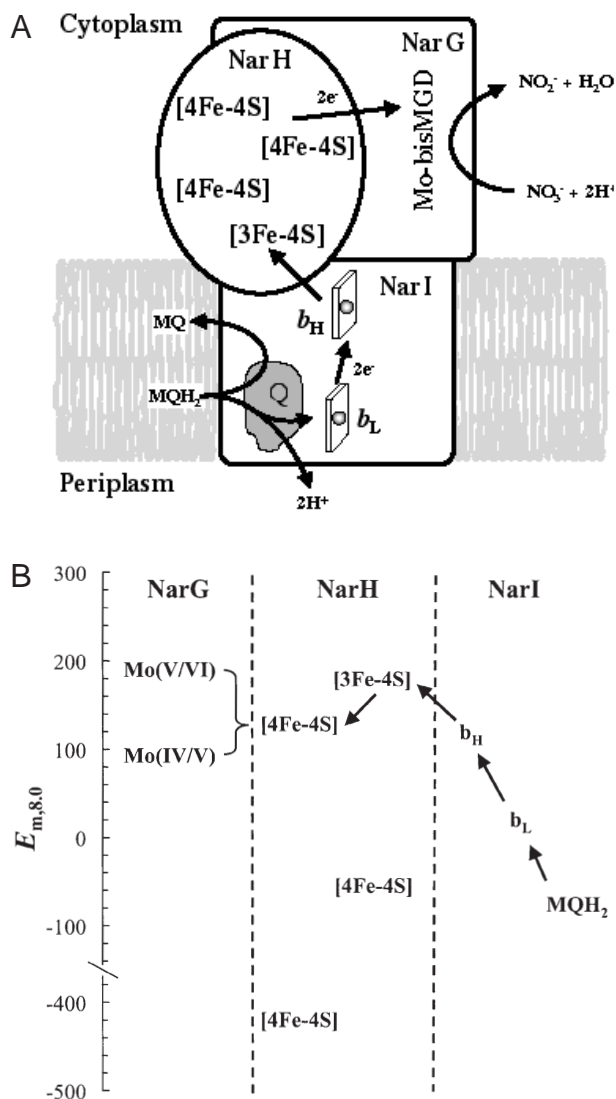


Figure 1. Overall topology and redox chemistry of NarGHI. A. Topological model of the enzyme showing its prosthetic group composition, overall electron-transfer pathway, and bioenergetics. Note that there is no experimental evidence to support the hypothesis (Breton *et al.*, 1994) that there is a fifth [Fe-S] cluster in NarG (Magalon *et al.*, 1998a; Rothery *et al.*, 1998b). B. Overall electrochemistry of the NarGHI prosthetic groups. Arrows indicate a plausible electron-transfer pathway based on experimental data (Magalon *et al.*, 1998a; Magalon *et al.*, 1997b; Rothery *et al.*, 1998b; Vincent and Bray, 1978).

et al., 1995b; Hacket and Bragg, 1982; Magalon *et al.*, 1997a; Magalon *et al.*, 1998b; Rothery *et al.*, 1999a). The NarG and NarH subunits (NarGH) comprise a membrane-extrinsic catalytic dimer that is anchored to the inner surface of the cytoplasmic membrane by NarI. Figure 1 summarizes the overall topology and thermodynamics of NarGHI.

Potentiometric analyses of NarGHI reveal that its prosthetic groups range in midpoint potential (E_m) from -400mV for the lowest potential [4Fe-4S] cluster to +180mV for the [3Fe-4S] cluster and the Mo(V/VI) couple of the Mo-bisMGD (Guigliarelli *et al.*, 1996; Rothery *et al.*, 1998b; Rothery *et al.*, 1999b; Vincent and Bray, 1978) (Figure 1). However, the E_m = -400mV [4Fe-4S] cluster is the only prosthetic group with a potential apparently too low to

undergo formal oxidation-reduction in an electron-transfer pathway from menaquinol (MQH₂, $E_{m,7}$ = -74mV) to nitrate ($E_{m,7}$ = +420mV). In other enzyme systems, for example in the *E. coli* and *Wolinella succinogenes* fumarate reductases (FrdABCD and FrdCAB), a low potential cluster has been identified (a [4Fe-4S] cluster, FR2) that appears to be directly on the electron-transfer conduit (Iverson *et al.*, 1999). Theoretical analyses of inter-centre electron tunnelling suggest that electron-transfer involving such low potential clusters can be high enough to support observed rates of catalytic turnover (Ohnishi *et al.*, 2000; Page *et al.*, 1999). It is therefore possible that the E_m = -400mV [4Fe-4S] cluster of NarGHI is part of the electron-transfer pathway through NarGHI. However, experimental evidence suggests that a mutant lacking this cluster is able to support respiratory growth on nitrate and retains significant quinol:nitrate oxidoreductase activity (Guigliarelli *et al.*, 1996). It is therefore possible that it plays an alternative role, for example in helping to define the structure of NarGHI, in particular of NarH. It has been proposed that there is an eighth prosthetic group in NarGHI, a [4Fe-4S] cluster coordinated by an N-terminal Cys motif in NarG (Berks *et al.*, 1995a; Breton *et al.*, 1994), but existing experimental evidence does not support this hypothesis (Magalon *et al.*, 1998a; Rothery *et al.*, 1998b; Trieber *et al.*, 1996).

NarI anchors NarGH to the inner surface of the cytoplasmic membrane (Blasco *et al.*, 1989; Chaudhry and MacGregor, 1983; Jones *et al.*, 1980; Magalon *et al.*, 1997a). It is also the site of quinol binding and oxidation, and provides an electron-transfer conduit from this functionality to the [Fe-S] clusters of NarH. Electron-transfer out of NarI is mediated by two hemes, one of relatively low E_m (+20mV, heme b_L), and one of relatively high E_m (+120mV, heme b_H) (Hacket and Bragg, 1982; Magalon *et al.*, 1997a; Rothery *et al.*, 1999a). NarI is of interest because: (i) it can be readily overexpressed to high levels in the cytoplasmic membrane, either as part of the NarGHI holoenzyme or by itself as NarI(Δ GH); (ii) it is susceptible to a number of well-characterized respiratory-chain inhibitors that bind to quinol binding sites (Q-sites); and (iii) it can be readily be mutagenized.

Sequence, Structure, and Heme Composition

A NarGHI-type enzyme has been identified in a range of bacterial species. Figure 2 shows ten NarI sequences aligned using the ClustalW alignment algorithm (Thompson *et al.*, 1994). The diversity of the sequences provides a convenient filter for the identification of important amino acid residues. Hydropathy analyses suggest the presence of five transmembrane helices (TM1-TM5), and the distribution of changes within the membrane-extrinsic loops (the "positive inside rule" (von Heijne, 1989)) suggests that there is a periplasmic amino-terminus and a cytoplasmic carboxy-terminus (Berks *et al.*, 1995b). The amino acid sequence of NarI is shown superimposed upon its proposed topology in Figure 3A. Highly conserved residues within the NarI family are shown in black, and the two hemes are coordinated between TM1 and TM5 by H56/H205 (heme b_H) and H66/H187 (heme b_L) (Magalon *et al.*, 1997a; Rothery *et al.*, 1999a). In addition, the overall

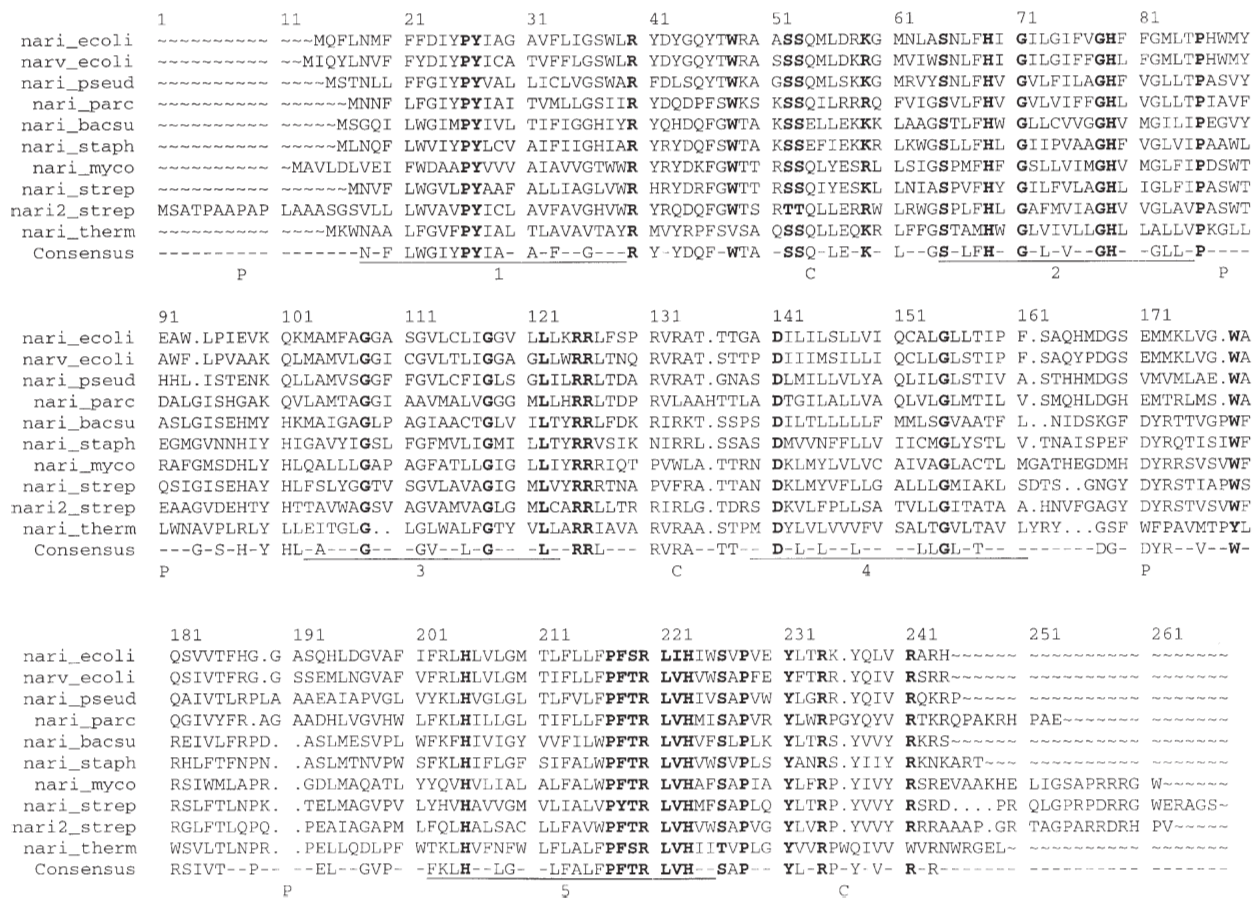


Figure 2. Sequence alignment of NarI subunits. NarI proteins were identified using the NETBLAST program of the Wisconsin Sequence Analysis Package (Version 9.1, Genetics Computer Group (GCG), Madison WI). Sequences were aligned using the CLUSTALW alignment algorithm (Thompson *et al.*, 1994). Key: *nari_ecoli*, *E. coli* NarI (accession no. P11350); *narv_ecoli*, second *E. coli* NarI (P19316); *nari_pseud*, *Pseudomonas aeruginosa* NarI (Y1252); *nari_parc*, *Paracoccus denitrificans* NarI (S61309); *nari_bacsu*, *B. subtilis* NarI (P42177); *nari_staph*, *Staphylococcus carnosus* NarI (AAC82545); *nari_myco*, *Mycobacterium tuberculosis* NarI (Z95584); *nari2_strep*, second *Streptomyces coelicolor* NarI (AL031515); *nari2_strep*, second *Streptomyces coelicolor* NarI (CAB53443); *nari_therm*, *Thermus thermophilus* NarI (Y10124). Putative transmembrane segments (Berks *et al.*, 1995b) are underlined and absolutely conserved residues are in bold type. P - periplasmic loop; C - cytoplasmic loop.

positions of the two putative Q-sites of NarGHI are indicated. These are the Q_P (Periplasmic) and Q_{Nr} (nitrate reductase) sites (Brito *et al.*, 1995; Magalon *et al.*, 1998b; Rothery *et al.*, 1999a) (see below for a description of an alternative nomenclature). In considering the proposed transmembrane topology of NarI presented in Figure 3A, it should be noted that the absolute length of the individual TM segments and the relative depth of individual residues within the membrane may differ significantly from the predictions of hydrophathy analyses, as has been observed in the structure of *E. coli* FrdABCD determined by X-ray crystallography (Iverson *et al.*, 1999).

Among hydrophobic diheme cytochromes *b*, much confusion reigns in the terminology used for both the hemes and the Q-sites. An emerging terminology for those enzymes with membrane-extrinsic catalytic subunits the sites and hemes based on their location relative to the membrane-extrinsic dimers (Iverson *et al.*, 1999; Lancaster *et al.*, 1999; Ohnishi *et al.*, 2000). In this system, heme *b_H* of NarGHI would become heme *b_P* (Proximal) and heme *b_L* would become heme *b_D* (Distal). Likewise the putative Q_{Nr} site would become the Q_P site and the Q_P site would become the Q_D site. However, in contrast to other systems,

a consistent terminology (Q_P/Q_{Nr}/*b_L*/*b_H*) has been in use for a number of years for the NarGHI system, and we therefore favour retaining it (Magalon *et al.*, 1997a; Magalon *et al.*, 1998b; Rothery *et al.*, 1999a). For clarity in comparisons between different diheme cytochrome *b* systems, we have indicated the alternative terminology (Q_D/Q_P/*b_D*/*b_P*) in the appropriate Figures (Figure 3A and Figure 7).

Figure 3B shows a plot of the overall sequence similarity in the alignment of Figure 2 versus residue position in combination with the proposed transmembrane topology of NarI (Figure 3A). Within the proposed TM segments, similarity peaks are located in TM1, TM2, and TM5. The observed similarity in TM2 and TM5 is consistent with these helices being the locations of the four His residues that coordinate the two hemes (Magalon *et al.*, 1997a; Rothery *et al.*, 1999a). The distribution of the similarity scores within the membrane-extrinsic loops can provide information on the transmembrane topology of NarI. Within the family of NarI sequences, above average similarity is observed in loop TM1-TM2 (putative cytoplasmic) and after the end of TM5 (putative cytoplasmic). Below average similarity is observed in loops

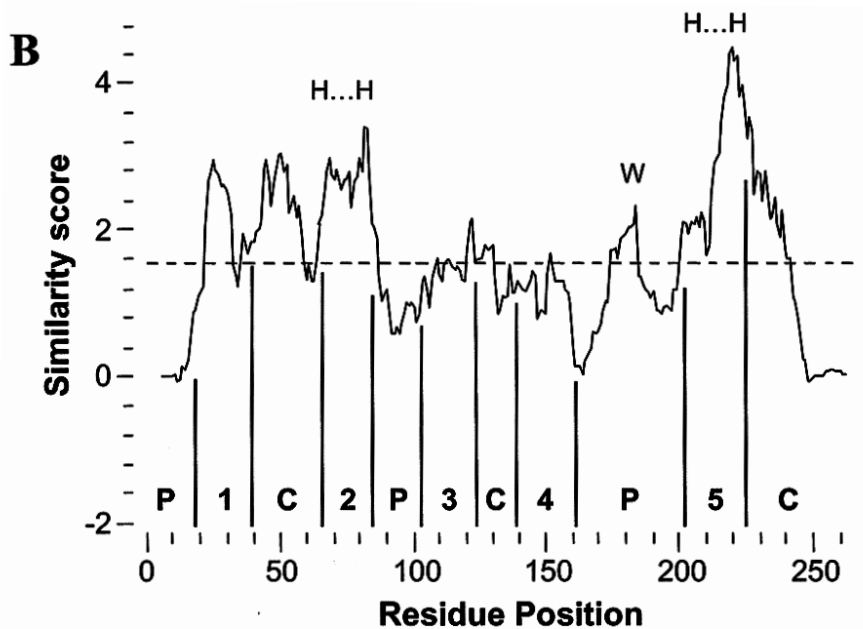
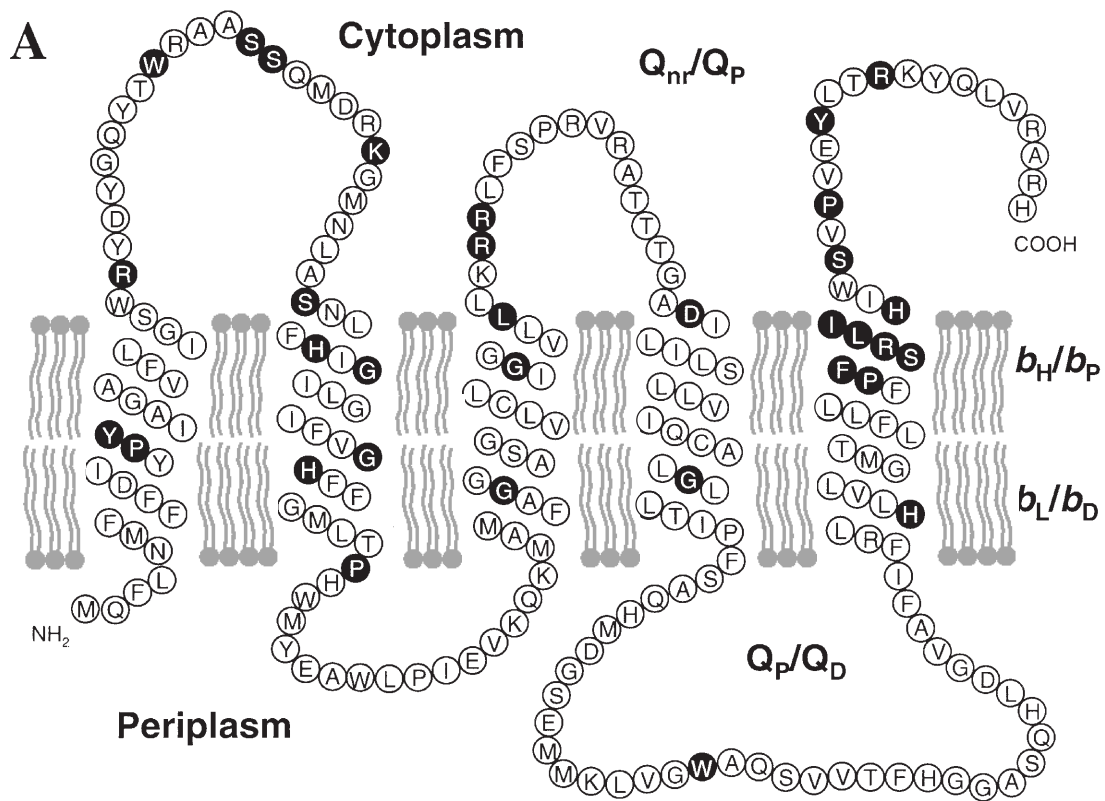


Figure 3. Transmembrane topology and plotsimilarity of the sequence of NarI. A. Amino acid sequence of NarI showing absolutely conserved residues (black circles) within the group of sequences presented in Figure 2. Q_p/Q_d - Periplasmically oriented or Distal Q-site that has been identified as being dissociable in inhibitor-binding experiments (Magalon *et al.*, 1998b; Rothery *et al.*, 1999a). Q_{nr}/Q_p - putative Q-site localized between heme b_H and the [3Fe-4S] cluster of NarH (Q_{nr} - nitrate reductase; Q_p - Proximal) (Brito *et al.*, 1995; Magalon *et al.*, 1997b). B. Plot of sequence similarity *versus* residue position of the sequence alignment of Figure 2 using a window average of 10. The positions of transmembrane segments 1-5 are indicated, as are the proposed locations of the extramembrane loops. The plot was generated using the PLOTSIMILARITY program of the Wisconsin Sequence Analysis Package in combination with the alignment of Figure 2. Note that residue numbering corresponds to that of the alignment of Figure 2.

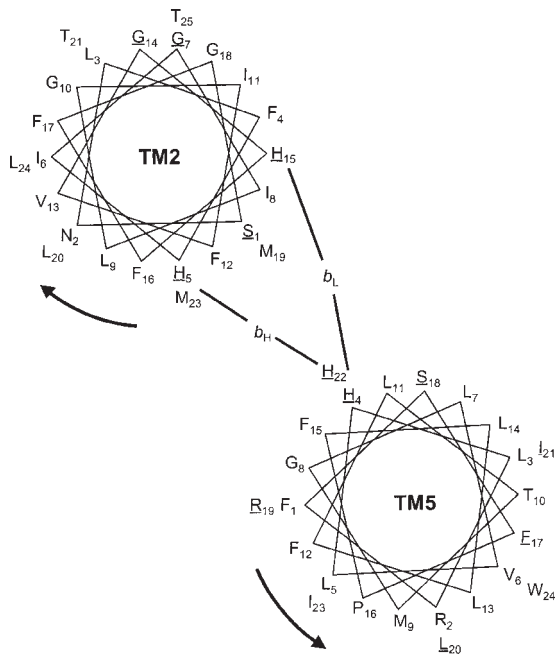


Figure 4. Helical wheel projections of putative transmembrane segments 2 and 5. Shown is the possible view looking away from the NarGH catalytic dimer. Residue numbering is from the start of the putative transmembrane segments identified in Figure 2. Absolutely conserved residues are underlined.

TM2-TM3 (putative periplasmic), TM3-TM4 (putative cytoplasmic), and TM4-TM5 (putative periplasmic). However, in the latter case there is a significant spike of similarity within this rather long periplasmic loop. These observations are consistent with the cytoplasmically localized similarity defining NarGH-NarI subunit interactions and an electron-transfer conduit. The spike within loop TM4-TM5 may define some other important functionality within NarI such as a Q-site.

Conserved His residues in the NarI sequence correspond to H56/H66 in TM2 and H187/H205 in TM5 and their role in heme coordination has been demonstrated by site-directed mutagenesis (Magalon, 1997; Magalon *et al.*, 1997a; Rothery *et al.*, 1999a). In the case of TM5, the two His residues are located on the same segment of the helix in a helical wheel projection (Figure 4). In TM2, the His residues fall in separate segments with approximately 80° between them on the vertical axis, implying that there is either: (a) a kink in one of the two heme-coordinating helices (most likely TM5), or; (b) a significant angle between the axis of the longer helix (TM5) and the membrane normal (and the axis of TM2). In this context, it should be noted that in proteins of known structure it is common for the helices to be tilted relative to the membrane normal (Iverson *et al.*, 1999; Lancaster, 1998; Xia *et al.*, 1997; Zhang *et al.*, 1998).

In NarGHI, the primary location of quinol binding and

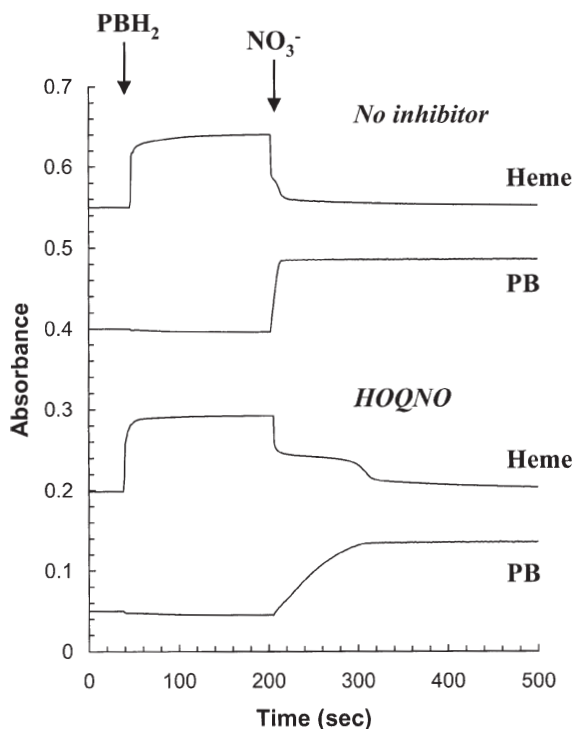


Figure 6. Use of reduced plumbagin to follow heme and quinol redox states in the presence of HOQNO. Membranes enriched in NarGHI (0.6mg mL⁻¹ protein) were incubated in N₂ saturated 100mM MOPS/5mM EDTA (pH7.0). 0.345mM reduced plumbagin (PBH₂) were added and the reduction of the hemes was followed by measuring the OD₅₆₀₋₅₇₅ (x1.0). The redox state of the PBH₂ was measured by following the OD₄₁₉₋₅₇₅ (x0.05). Subsequent oxidation was accomplished by adding 17mM KNO₃. Where indicated, HOQNO was added to a concentration of 34μM HOQNO.

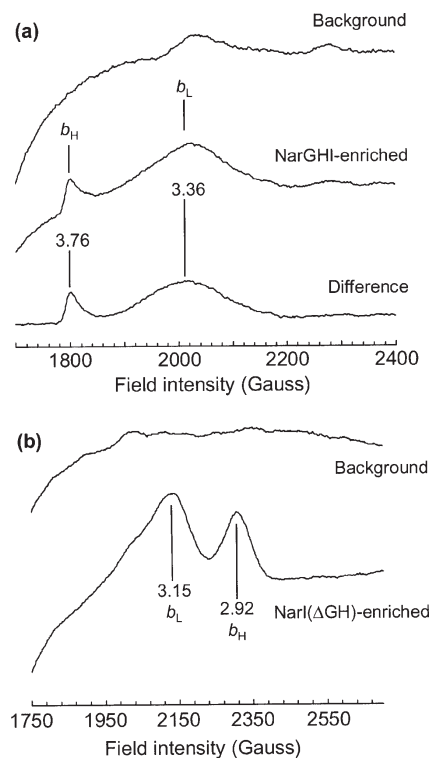


Figure 5. EPR spectra of NarGHI (a) and NarI(ΔGH) (b) in *E. coli* inner membranes. Spectra were recorded at a temperature of 12K with a modulation amplitude of 20G_{pp} at a microwave power of 20mW for (a) and 2mW for (b).

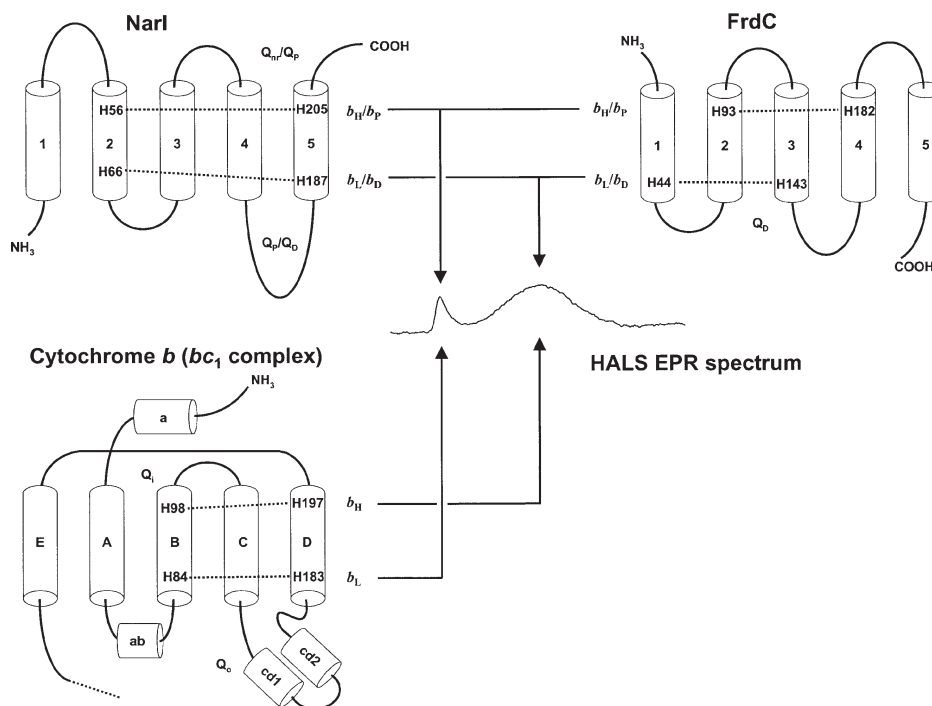


Figure 7. Comparison of NarI with membrane-bound cytochromes *b* of known structure. The topology presented for NarI is a simplified version of that presented in Figure 3A, emphasizing heme coordination and possible Q-sites. The topology of FrdC is that from *W. succinogenes* FrdCAB based on its crystal structure (Lancaster, 1998). The topology of cytochrome *b* (*bc*₁ complex) is a subset of that presented by Zhang *et al.* (Zhang *et al.*, 1998) with helices F1, F2, G, and H omitted for clarity. The cytoplasmic side of the membrane is located above each protein. The indicated positions of the Q_i and Q_o Q-sites are approximate and cannot be considered accurate in a two-dimensional representation of the transmembrane structure. Note that for NarI and FrdC electrons are transferred to a cytoplasmically-localized electron-transfer subunit that is proximal to heme *b*_H, whereas in the case of cytochrome *b* electron transfer is bifurcated from Q_o to *b*_L→*b*_H→Q_i and to the Rieske [2Fe-2S] cluster.

oxidation appears to be located towards the periplasmic side of NarI (the Q_P site) in close association with heme *b*_L (Magalon *et al.*, 1997a; Magalon *et al.*, 1998b; Rothery *et al.*, 1999a). However, almost all of the sequence conservation identified in Figures 2, 3, and 4 lies towards the cytoplasmic side of the membrane. The exception to this is in the rather long loop between TM4 and TM5. In particular, there is a conserved Trp residue (W162) that appears in all the sequences of Figure 2 with the exception of the NarI subunit of *Thermus thermophilus*, where it is replaced with a Tyr residue. Such a highly conserved Trp residue plays an important role in the proximal (Q_P^{FRD}) site of *E. coli* FrdABCD (Iverson *et al.*, 1999; Westenberg *et al.*, 1993) and a number of other Q-sites (Murray *et al.*, 1999). Given the generally very weak sequence conservation associated with Q-sites in different enzyme systems (Fisher and Rich, 2000), it is possible that the spike in sequence similarity in the TM4-TM5 loop may play a role in defining the Q_P site.

Within the TM segments, a number of additional residues warrant mention. There are five Gly residues that are absolutely conserved, comprising pairs in TM2 and TM3, and a single Gly in TM4 (Figures 2 and 3A). In complex III at least one of the conserved Gly residues is involved in the packing of heme *b*_L into the cytochrome *b* subunit (Saribas *et al.*, 1997). In the helical wheel projection of Figure 4, the two conserved Gly residues in TM2 are almost on the opposite side of the helix from the heme-coordinating His residues, so are unlikely to have such a

role. But the two Gly residues in TM3 and the conserved Gly in TM4 might be involved in accommodating the hemes. In TM5 of NarI, in addition to the two conserved heme-coordinating His residues, there is a sequence towards the cytoplasmic end of the segment (PFSRLIHxxSxPxxYxxR) that is highly conserved that includes one of the heme ligands (H205). Thus, consideration of the sequence identity within the family of NarI proteins identifies a number of residues beyond the heme-coordinating His residues as targets for mutagenesis. These include the Trp in loop TM4-TM5 (putative Q_P-site), Gly residues within TM3 and TM4 (putative heme packing), and the highly conserved sequence at the cytoplasmic end of TM5.

EPR Spectroscopy of the Two Hemes

Although the hemes of NarGHI have optical spectra typical of low-spin cytochromes *b* (Hacket and Bragg, 1982; Magalon *et al.*, 1997a), it has been through the application of EPR spectroscopy that significant advances have been made in understanding their structure and function. This is because low-spin hemes *b* have overlapping optical spectra that can be difficult to deconvolute, whereas they typically have clearly resolved EPR spectra. This advantage has also been exploited in other proteins having multiple low-spin hemes *b* such as the SdhC subunit of *Bacillus subtilis* succinate dehydrogenase (Hägerhäll *et al.*, 1992; Hägerhäll *et al.*, 1995a) and the cytochrome *b* subunit of complex III

(Salerno, 1984; Saribas *et al.*, 1997; Valkova-Valchanova *et al.*, 1998).

High level protein overexpression (to ~50% of the inner membrane protein) has allowed intensive scrutiny of the hemes of NarGHI *in situ* (Magalon, 1997; Magalon *et al.*, 1997a; Magalon *et al.*, 1998b; Rothery *et al.*, 1999a). The NarGHI hemes are low-spin (six-coordinate iron) and exhibit EPR spectra with features typical of HALS (highly anisotropic low-spin) hemes (Walker *et al.*, 1986), in which there is a large imidazole ligand interplanal angle (Dou *et al.*, 1995). In this type of heme, only one of the three g_z tensors (g_z) is observed by EPR (Salerno, 1984). Figure 5a shows the deconvoluted EPR spectrum of the two hemes, showing features at $g_z=3.36$ and $g_z=3.76$. This spectrum is reminiscent of that of the hemes *b* of complex III (Salerno, 1984; Valkova-Valchanova *et al.*, 1998), and the proposed model for Narl heme coordination (Figure 3A) is superficially similar to that seen in the structure of complex III (Xia *et al.*, 1997; Zhang *et al.*, 1998), with the two hemes being coordinated between two transmembrane helices.

Site-Directed Mutagenesis of Heme-Coordinating His Residues

Assignment of the His ligands of hemes b_L and b_H in NarGHI is based on EPR/optical studies of four site-directed mutants, NarGHI^{H56R}, NarGHI^{H66Y}, NarGHI^{H187Y}, and NarGHI^{H205Y} (Magalon, 1997; Magalon *et al.*, 1997a). The ligands for hemes b_L and b_H are H66/H187 and H56/H205, respectively, in agreement with the sequence conservation of these residues (Figure 2) (Berks *et al.*, 1995b). This strongly supports the model for the overall topology of Narl presented in Figure 3.

Loss of heme b_L causes readily interpretable changes in the properties of NarGHI (loss of the corresponding EPR signal and loss of quinol binding and oxidation) with few consequences for the remaining prosthetic groups of NarGHI (Magalon *et al.*, 1997a; Rothery *et al.*, 1999a). In contrast, loss of heme b_H in NarGHI^{H56R} causes: (i) a decrease in the anisotropy (g_z) of heme b_L (Magalon *et al.*, 1997a); (ii) an increase in the E_m of heme b_L (Rothery *et al.*, 1999a), and; (iii) an alteration in the EPR spectrum of the [3Fe-4S] cluster of NarH. The first two observations can be rationalized on the basis that both hemes are coordinated between TM2 and TM5 of Narl, and any conformational effects could easily be transferred via these two transmembrane helices. For example, in complex III, loss of heme b_H also increases the E_m of heme b_L (Yun *et al.*, 1991). The effect of the loss of heme b_H on the NarH [3Fe-4S] cluster suggests that this cluster and the heme are located close to the NarH-Narl interface. This is consistent with experimental and structural data on three other enzyme systems. (i) In the crystal structure of *E. coli* FrdABCD (Iverson *et al.*, 1999), the [3Fe-4S] cluster (FR3) of FrdB is located close to the FrdCD-FrdB interface. A number of residues of FrdB are located within 5Å of the proximal MQ binding site (Q_P^{FRD}), and FR3 is located ~11Å from this site. (ii) In *W. succinogenes* fumarate reductase (FrdCAB), the distance between FR3 and the edge of the proximal heme (heme b_P) is also ~11Å (Lancaster *et al.*, 1999). (iii) In *E. coli* DMSO reductase (DmsABC), a

[4Fe-4S] cluster of DmsB that is essential for MQH₂ oxidation is located close to a Q-site in DmsC (Q_P^{DMS}) and has also been localized close to the DmsB-DmsC interface (Rothery and Weiner, 1991; Rothery and Weiner, 1993; Rothery and Weiner, 1996). Thus, in NarGHI, it is possible that heme b_H is in a location similar, relative to the electron-transfer subunit, to the Q_P^{FRD}/Q_P^{DMS} site of FrdABCD/DmsABC and the heme b_P of *W. succinogenes* FrdCAB. Overall, these data support the topology of Narl presented in Figure 3A with hemes b_H and b_L being located towards the cytoplasmic and periplasmic sides of the membrane, respectively.

When Narl is expressed and assembled into the cytoplasmic membrane in the absence of NarGH (Narl(Δ GH)), its low-spin heme EPR spectrum is dramatically altered compared to that of the holoenzyme (Magalon *et al.*, 1997b; Magalon *et al.*, 1998b). The EPR spectrum of Narl(Δ GH) (Figure 5b) exhibits two g_z features attributable to low-spin ferric heme, one at $g_z=3.15$, and another with a $g_z=2.92$. On the basis of its inhibitor-sensitivity, the $g_z=3.15$ feature can be assigned to heme b_L (Magalon *et al.*, 1998b). The observation of a $g_z=2.92$ feature may correlate with an almost parallel imidazole ligand orientation (Dou *et al.*, 1995; Walker *et al.*, 1986), indicating that a "relaxation" in the environment of this heme occurs in the absence of NarGH, as has been observed in the membrane anchors of mitochondrial and *E. coli* succinate dehydrogenase (Yang *et al.*, 1997; Yu *et al.*, 1987). The $g_z=2.92$ feature of the spectrum is eliminated in Narl(Δ GH)^{H56R}, unequivocally assigning it to a "relaxed" form of heme b_H (Rothery *et al.*, 1999a). The E_m of heme b_L in Narl(Δ GH) is +37mV, which is a modest increase from the value of +20 observed in NarGHI (Rothery *et al.*, 1999a). Surprisingly, the E_m of heme b_H drops from +120mV in NarGHI to -178mV in Narl(Δ GH), a ΔE_m of almost -300mV. In chloroplast cytochrome b_{559} exposure of the heme to the aqueous milieu results in a large negative ΔE_m (Krishtalik *et al.*, 1993), suggesting that the absence of the NarGH results in a similar exposure of heme b_H in Narl(Δ GH). This is further evidence for the localization of heme b_H to the NarH-Narl interface region of NarGHI.

Q-Site Inhibitors

NarGHI is able to use both menaquinol (MQH₂) and ubiquinol (UQH₂) as physiological reductants (Giordani *et al.*, 1997; Guigliarelli *et al.*, 1996; Wallace and Young, 1977). Significant progress in studies of quinol binding has been made using quinol analog substrates and inhibitors in combination with optical, fluorescence and EPR spectroscopies. Of a range of Q-site inhibitors of complex III tested (Magalon *et al.*, 1998b), only HOQNO and stigmatellin inhibit NarGHI with a sufficiently low I_{50} for them to be useful for further biochemical/biophysical studies. HOQNO binding to NarGHI renders heme b_L more anisotropic (g_z increases to ~3.50), suggesting that it increases the imidazole ligand interplanal angle (this is the angle between the planes of the imidazole rings measured along the imidazole nitrogen-iron-imidazole nitrogen axis) (Rothery *et al.*, 1999a; Walker *et al.*, 1986). Stigmatellin also binds in the vicinity of heme b_L , but in this case there is a decrease in anisotropy, suggesting a decrease in the

imidazole ligand interplanal angle. These contrasting effects on the possible imidazole interplanal angle may explain the different effects of these inhibitors on the E_m values of the two hemes. HOQNO causes a near reversal of the E_m values (a positive ΔE_m for heme b_L and a negative ΔE_m for heme b_H), whereas stigmatellin elicits a modest positive ΔE_m on heme b_L and has no effect on heme b_H (Rothery *et al.*, 1999a). Since neither inhibitor has an effect on the EPR spectrum of heme b_H and both inhibitors affect the E_m of heme b_L , it is clear that there is at least one Q-site (the Q_P site) located in the vicinity of the latter heme. The large negative ΔE_m elicited by HOQNO on heme b_H suggests either that a conformational change is propagated to this heme via the heme b_L and TM2/TM5, or that there is another site of HOQNO binding in the vicinity of heme b_H .

The determination of the number of dissociable HOQNO binding sites (and presumably MQH₂/UQH₂ binding sites) was achieved through the use of fluorescence quench titrations (Brandt and von Jagow, 1991; Okun *et al.*, 1999; van Ark and Berden, 1977). HOQNO binding to NarGHI occurs with a K_d of $\sim 0.2\mu\text{M}$ at a single site that is sensitive to the absence of heme b_L , but not to the absence of heme b_H (Rothery *et al.*, 1999a). This site appears to overlap with, or be sterically hindered by, the site for stigmatellin binding. The absence of NarGH in NarI(Δ GH) does not appear to affect HOQNO binding. Thus, a combination of EPR and fluorescence spectroscopies point to a model for quinol binding in which there is a single dissociable high-affinity site (the Q_P site) located towards the periplasmic side of NarI in close proximity to heme b_L . This model is consistent with the proposed bioenergetics of NarGHI in which scalar protons from MQH₂ oxidation are released into the periplasm during enzyme turnover (Berks *et al.*, 1995b; Jones *et al.*, 1980).

There is evidence suggesting that a second Q-site exists in NarGHI (the Q_{nr} site). During nitrate-induced enzyme turnover, an HOQNO-sensitive radical species is observed that is likely to be located in the vicinity of the NarH [3Fe-4S] cluster (Magalon *et al.*, 1997b). It has been proposed that this species is a menasemiquinone anion that arises from a tightly bound MQ-9 that copurifies with the NarGH catalytic dimer (Brito *et al.*, 1995; Magalon *et al.*, 1997b). Also, HOQNO and stigmatellin inhibit nitrate-dependent heme reoxidation (Magalon *et al.*, 1998b) (Figure 6), suggesting the presence of a second dissociable Q-site between heme b_H and the [3Fe-4S] cluster (the Q_{nr} site). This site would perhaps be similar to the Q_P^{FRD} (Iverson *et al.*, 1999) and Q_P^{DMS} sites (Rothery and Weiner, 1991; Rothery and Weiner, 1993; Rothery and Weiner, 1996). However, in contrast to what is observed with FrdABCD (Hägerhäll *et al.*, 1999; Rothery and Weiner, 1998), HOQNO elicits no effect on EPR properties of the [3Fe-4S] cluster of NarH (Rothery *et al.*, 1999a). It is possible that the observed inhibition of heme reoxidation in NarGHI is due to bound inhibitor (at the Q_P site) preventing oxidation of heme b_L (in the case of HOQNO, the ΔE_m elicited on heme b_L is entirely consistent with this possibility). It should also be noted that the presence of a dissociable Q_{nr} site would be difficult to reconcile with the proposed bioenergetics of NarGHI (Berks *et al.*, 1995b; Jones *et al.*, 1980), as it would presumably result in the

release of protons on both the periplasmic and cytoplasmic faces of NarI, reducing the H^+/e^- ratio for enzyme turnover. In fact, the proton gradient across the cytoplasmic membrane would favor quinol oxidation and proton release at the putative Q_{nr} site over the Q_P site.

A more compelling explanation for the data that has been used to suggest the presence of a dissociable Q_{nr} site is that inhibitors such as HOQNO and stigmatellin bind with much higher affinity to the reduced form of the enzyme than to the oxidized form. Thus, when the reduced enzyme is subjected to nitrate-induced oxidation, oxidation of heme b_L has to await dissociation of inhibitor from the Q_P site. This would explain the apparent inhibition of heme reoxidation shown in Figure 6 and elsewhere (Magalon *et al.*, 1998b). In the data presented in Figure 6, the rapid first phase of nitrate-dependent reoxidation in the presence of HOQNO is likely to correspond to heme b_H oxidation, whereas the second slower phase is likely to correspond to heme b_L oxidation. This second phase appears to occur following exhaustion of reduced quinol substrate (plumbagin).

Quinol binding and oxidation by NarGHI has also been addressed by steady-state enzymology. When the hydroxylated naphthoquinols reduced lapachol and plumbagin are used as substrates, kinetics are observed that are consistent with binding to a single site within the NarGHI complex (Rothery *et al.*, 1998a). However, a more complex analysis (Giordani *et al.*, 1997) suggests the presence of two quinol binding sites, one which preferentially binds a MQH₂ analog and another which preferentially binds a UQH₂ analog (i.e. the analyses suggests two sites for both MQH₂ and UQH₂ analogs). However, in another steady-state kinetics study, (Morpeh and Boxer, 1985) the data was consistent with only a single dissociable Q-site (for UQH₂). Thus, at the present time, not all the kinetic data agrees with the EPR/fluorescence data suggesting only a single dissociable Q_P site in the vicinity of heme b_L .

In the context of identifying the number of Q-sites in NarGHI, it is important to distinguish between dissociable and non-dissociable sites. For example, the MQ-9 identified in purified NarGHI dimer (Brito *et al.*, 1995) could reside at a non-dissociable Q-site in a position equivalent to the proposed Q_{nr} site. Such a non-dissociable quinol species has been identified in *E. coli* cytochrome *bo* (Ingledew *et al.*, 1995; Sato-Watanabe *et al.*, 1995; Sato-Watanabe *et al.*, 1994), as well as in the well-characterized bacterial photoreaction centre (the so-called Q_A site) (Allen and Williams, 1998; Ermler *et al.*, 1994).

Comparison with Other Diheme Membrane-Bound Cytochromes *b*

Figure 7 illustrates the overall topology of NarI in comparison with two hydrophobic diheme cytochromes *b* of known structure: the cytochrome *b* subunit of mitochondrial complex III (Xia *et al.*, 1997; Zhang *et al.*, 1998) and the FrdC subunit of *W. succinogenes* fumarate reductase (FrdCAB) (Lancaster *et al.*, 1999). The latter enzyme has considerable sequence, and inferred structural similarity with *B. subtilis* succinate dehydrogenase (SdhCAB) (Hägerhäll, 1997; Hägerhäll and Herderstedt,

1996). Also shown is the correlation between the hemes of the proteins and their inferred EPR anisotropy. In the models presented in Figure 7, the cytoplasmic side of the membrane and the membrane-extrinsic catalytic dimers of NarGHI/FrdCAB are located above each protein model. In the case of the cytochrome *b* subunit of complex III, electrons from quinol oxidation are passed to a Rieske [Fe-S] protein located on the periplasmic side of the complex (below the cytochrome *b* model of Figure 7).

The structure of the cytochrome *b* subunit of complex III provides a good model for the coordination of two hemes *b* by four His residues in two transmembrane helices (Xia *et al.*, 1997; Zhang *et al.*, 1998). Both hemes *b* have architypical HALS EPR lineshapes (Salerno, 1984; Walker *et al.*, 1986), are located approximately 20 Å apart (Fe-Fe distance) (Xia *et al.*, 1997), and appear to undergo the same type of long-range redox interactions as are observed between the hemes of NarI (Howell and Robertson, 1993; Rothery *et al.*, 1999a). However, there are significant differences between the hemes *b* of NarI and those of complex III:

(i) In complex III, the more anisotropic g_z has been assigned to heme b_L , whereas the less anisotropic g_z has been assigned to heme b_H . In mouse complex III, these hemes have E_m values of approximately -31 (b_L) and 92mV (b_H), respectively (Howell and Robertson, 1993). In NarGHI, the more anisotropic heme ($g_z=3.76$; b_H) has an E_m of approximately 120mV and the less anisotropic heme ($g_z=3.36$; b_L) has a E_m of approximately 20mV (Hackett and Bragg, 1982; Magalon *et al.*, 1997a; Rothery *et al.*, 1999a). Thus, in NarGHI, it is the higher potential heme that is most anisotropic, whereas in complex III it is the lower potential heme.

(ii) Present evidence suggests the presence of only a single dissociable Q-site in NarI (the Q_P site), whereas in complex III there are regions of dissociable quinone/quinol binding oriented towards opposite sides of the cytochrome *b* subunit (Xia *et al.*, 1997).

(iii) In the structure of complex III, two of the TM segments (B and D, of a total of eight) provide heme ligands, but these run in the same direction (inward, towards the mitochondrial matrix/bacterial cytoplasm) (Zhang *et al.*, 1998), whereas in NarI the equivalent helices (TM2 and TM5) are antiparallel.

The membrane anchor subunit of *W. succinogenes* FrdCAB (Lancaster *et al.*, 1999), although being a five TM segment diheme cytochrome *b*, is clearly structurally distinct from NarI. In this case, four rather than two of the helices coordinate the hemes via His residues. The proximal heme of FrdCAB (heme b_P) is coordinated between TM2 and TM4, whilst the distal heme (heme b_D) is coordinated between TM1 and TM3 (Lancaster *et al.*, 1999). This results in an interplanal angle for the two hemes of 95°. The membrane anchor of *W. succinogenes* FrdCAB is likely to be very similar in overall structure to that of the succinate dehydrogenase of *B. subtilis* succinate dehydrogenase (SdhCAB) (Hägerhäll, 1997). In the latter case, it has been shown that HOQNO elicits a large negative ΔE_m on heme b_L (equivalent to heme b_D of *W. succinogenes* FrdC), but has no effect on the E_m of heme b_H (equivalent to heme b_P of *W. succinogenes* FrdC) (Smirnova *et al.*, 1995) or the [3Fe-4S] cluster of SdhB

(Hägerhäll *et al.*, 1995b). These observations are consistent with the long-range redox interactions observed between the hemes of NarI being propagated via the two heme-coordinating TM segments.

In NarGHI and *B. subtilis* SdhCAB, it is the more anisotropic heme (b_H -NarGHI; b_P -SdhCAB) that is close to the interface between the membrane anchor (NarI/SdhC) subunit and the electron-transfer subunit (Hägerhäll *et al.*, 1992; Magalon *et al.*, 1997a; Rothery *et al.*, 1999a). It is very likely that in *W. succinogenes* FrdCAB, heme b_P is the more anisotropic heme. As described above, the environment of heme b_H of NarI is significantly altered in the absence of the membrane-extrinsic dimer. In *B. subtilis* SdhC in the absence of SdhAB, the EPR signal corresponding to heme b_P is not observed, suggesting that this heme is absent in the absence of the membrane-extrinsic subunits (Fridén *et al.*, 1990; Hederstedt and Andersson, 1986). Given these observations, it is likely that the interaction between the membrane anchor subunit and the electron-transfer subunit plays a large role in defining the environment of heme b_H (NarGHI) and heme b_P (FrdCAB/SdhCAB). It is also of note that in complex III, the most anisotropic heme is that one that is closest to the membrane-extrinsic Rieske [Fe-S] protein subunit. However, due to the overall complexity of complex III, in this case the correlation may be simply coincidental.

Conclusions and Outlook

Much recent progress has been made towards an understanding of the structure and function of NarI. At present, the majority of the data can only be interpreted in terms of a two dimensional model for its overall structure in which the highest resolution information relates to the overall number and orientation of the TM segments and estimates of the overall positions of the two hemes and putative Q-sites with respect to the membrane and the other prosthetic groups of NarGHI. What is now clearly necessary is an intensive effort to determine the structure of NarGHI or NarI(Δ GH) at atomic resolution. Recent successes in determining the structures of a number of membrane-bound, multisubunit, multifactor enzymes (Iverson *et al.*, 1999; Lancaster *et al.*, 1999; Xia *et al.*, 1997; Zhang *et al.*, 1998) suggests that success with NarGHI will soon be forthcoming. In addition, careful analyses of the sequence of *E. coli* NarI in comparison with other members of the NarI family of proteins suggest a number of residues suitable for site-directed mutagenesis and subsequent study. Both the structure-solving and mutagenesis approaches are in progress in our laboratories.

Acknowledgements

This work was funded by a grant from the Medical Research Council of Canada to J.H.W. (PG11440) and by the Centre National de la Recherche Scientifique. F.B. was supported by a travel grant from the Alberta Heritage Foundation for Medical Research.

References

- Allen, J.P., and Williams, J.C. 1998. Photosynthetic reaction centers. FEBS Lett. 438: 5-9.
- Augier, V., Asso, M., Guigliarelli, B., More, C., Bertrand, P., Santini, C., Blasco, F., Chippaux, M., and Giordano, G. 1993a. Removal of the high-potential [4Fe-4S] center of the β -subunit from *Escherichia coli* nitrate

- reductase. Physiological, biochemical, and EPR characterization of site-directed mutated enzymes. *Biochemistry*. 32: 5099-5108.
- Augier, V., Guigliarelli, B., Asso, M., Bertrand, P., Frixon, C., Giordano, G., Chippaux, M., and Blasco, F. 1993b. Site-directed mutagenesis of conserved cysteine residues within the β subunit of *Escherichia coli* nitrate reductase. Physiological, biochemical, and EPR characterization of the mutated enzymes. *Biochemistry*. 32: 2013-2023.
- Berks, B.C., Ferguson, S.J., Moir, J.W.B., and Richardson, D.J. 1995a. Enzymes and associated electron transport systems that catalyze the respiratory reduction of nitrogen oxides and oxyanions. *Biochim. Biophys. Acta*. 1232: 97-123.
- Berks, B.C., Page, M.D., Richardson, D.J., Reilly, A., Cavill, A., Outen, F., and Ferguson, S.J. 1995b. Sequence analysis of subunits of the membrane-bound nitrate reductase from a denitrifying bacterium: the integral membrane subunit provides a prototype for the diheme electron-carrying arm of a redox loop. *Mol. Micro*. 15: 319-331.
- Blasco, F., Iobbi, C., Giordano, G., Chippaux, M., and Bonnefoy, V. 1989. Nitrate reductase of *Escherichia coli*: completion of the nucleotide sequence of the *nar* operon and reassessment of the role of the alpha and beta subunits in iron binding and electron transfer. *Molec. Gen. Genet*. 218: 249-256.
- Blasco, F., Iobbi, C., Ratouchniak, J., Bonnefoy, V., and Chippaux, M. 1990. Nitrate reductases of *Escherichia coli*: sequence of the second nitrate reductase and comparison with that encoded by the *narGHJ* operon. *Mol. Gen. Genet*. 222: 104-111.
- Brandt, U., and von Jagow, G. 1991. Analysis of inhibitor binding to the mitochondrial cytochrome *c* reductase by fluorescence quench titration. Evidence for a 'catalytic switch' at the Q_0 center. *Eur. J. Biochem*. 195: 163-170.
- Breton, J., Berks, B.C., Reilly, A., Thomson, A.J., Ferguson, S.J., and Richardson, D.J. 1994. Characterization of the paramagnetic iron-containing redox centres of *Thiosphaera pantotropha* periplasmic nitrate reductase. *FEBS Lett*. 345: 76-80.
- Brito, F., DeMoss, J.A., and Dubourdieu, M. 1995. Isolation and identification of menaquinone-9 from purified nitrate reductase of *E. coli*. *J. Bacteriol*. 177: 3728-3735.
- Chaudhry, G.R., and MacGregor, C.H. 1983. Cytochrome *b* from *Escherichia coli* nitrate reductase. Its properties and association with the enzyme complex. *J. Biol. Chem*. 258: 5819-5827.
- Dou, Y., Admiraal, S.J., Ikeda-Saito, M., Krzywdza, S., Wilkinson, A.J., Li, T., Olson, J.S., Prince, R.C., Pickering, I.J., and George, G.N. 1995. Alteration of axial coordination by protein engineering in myoglobin. Bisimidazole ligation in the His⁶⁴Val/Val⁶⁹His double mutant. *J. Biol. Chem*. 270: 15993-16001.
- Ermier, U., Michel, H., and Schiffer, M. 1994. Structure and function of the photosynthetic reaction center from *Rhodobacter sphaeroides*. *J. Bioenerget. Biomem*. 26: 5-15.
- Fisher, N., and Rich, P.R. 2000. A motif for quinone binding sites in respiratory and photosynthetic systems. *J. Mol. Biol*. 296: 1153-1162.
- Fridén, H., Cheesman, M.R., Hederstedt, L., Andersson, K.K., and Thomson, A.J. 1990. Low temperature EPR and MCD studies on cytochrome *b*₅₅₈ of the *Bacillus subtilis* succinate:quinone oxidoreductase indicate bis-histidine coordination of the heme iron. *Biochim. Biophys. Acta*. 1041: 207-215.
- Giordano, R., Buc, J., Cornish-Bowden, A., and Cárdenas, M.L. 1997. Kinetics of membrane-bound nitrate reductase A from *Escherichia coli* with analogs of physiological electron donors. Different reaction sites for menadiol and duroquinol. *Eur. J. Biochem*. 250: 567-577.
- Guigliarelli, B., Asso, M., More, C., Augier, V., Blasco, F., Pommier, J., Giordano, G., and Bertrand, P. 1992. EPR and redox characterization of the iron-sulfur centres in nitrate reductases A and Z from *Escherichia coli*. Evidence of a high and low potential class and their relevance in the electron-transfer mechanism. *Eur. J. Biochem*. 207: 61-68.
- Guigliarelli, B., Magalon, A., Asso, M., Bertrand, P., Frixon, C., Giordano, G., and Blasco, F. 1996. Complete coordination of the four Fe-S centres of the β subunit from *Escherichia coli* nitrate reductase. Physiological, biochemical and EPR characterization of site-directed mutants lacking the highest or lowest potential [4Fe-4S] clusters. *Biochemistry*. 35: 4828-4836.
- Hackett, N.R., and Bragg, P.D. 1982. The association of two distinct *b* cytochromes with respiratory nitrate reductase of *Escherichia coli*. *FEMS Micro. Lett*. 13: 213-217.
- Hägerhäll, C. 1997. Succinate:quinone oxidoreductases. Variations on a conserved theme. *Biochim. Biophys. Acta*. 1320: 107-141.
- Hägerhäll, C., Aasa, R., von Wachenfeldt, C., and Hederstedt, L. 1992. Two hemes in *Bacillus subtilis* succinate:menaquinone oxidoreductase (complex II). *Biochemistry*. 31: 7411-7421.
- Hägerhäll, C., Fridén, H., Aasa, R., and Hederstedt, L. 1995a. Transmembrane topology and axial ligands to hemes in the cytochrome *b* subunit of *Bacillus subtilis* succinate:menaquinone reductase. *Biochemistry*. 34: 11080-11089.
- Hägerhäll, C., and Hederstedt, L. 1996. A structural model for the membrane-integral domain of succinate:quinone oxidoreductases. *FEBS Lett*. 389: 25-31.
- Hägerhäll, C., Magnitsky, S., Sled, V.D., Schröder, I., Gunsalus, R.P., Cecchini, G., and Ohnishi, T. 1999. An *Escherichia coli* mutant quinol:fumarate reductase contains an EPR-detectable semiquinone stabilized at the proximal quinone-binding site. *J. Biol. Chem*. 274: 26157-26164.
- Hägerhäll, C., Sled, V., Hederstedt, L., and Ohnishi, T. 1995b. The trinuclear iron-sulfur cluster S3 in *Bacillus subtilis* succinate:menaquinone reductase; effects of a mutation in the putative cluster ligation motif on enzyme activity and EPR properties. *Biochim. Biophys. Acta*. 1229: 356-362.
- Hederstedt, L., and Andersson, K.K. 1986. Electron-paramagnetic-resonance spectroscopy of *Bacillus subtilis* cytochrome *b*₅₅₈ in *Escherichia coli* membranes and in succinate dehydrogenase complex from *Bacillus subtilis* membranes. *J. Bacteriol*. 167: 735-739.
- Howell, N., and Robertson, D.E. 1993. Electrochemical and spectral analysis of the long range interactions between the Q_0 and Q_i sites and the heme prosthetic groups of ubiquinol-cytochrome *c* oxidoreductase. *Biochemistry*. 32: 11162-11172.
- Inglede, W.J., Ohnishi, T., and Salerno, J.C. 1995. Studies on a stabilization of ubisemiquinone by *Escherichia coli* quinol oxidase, cytochrome *bo*. *Eur. J. Biochem*. 227: 903-908.
- Iverson, T.M., Luna-Chavez, C., Cecchini, G., and Rees, D.C. 1999. Structure of the *Escherichia coli* fumarate reductase respiratory complex. *Science* 284: 1961-1966.
- Jones, W.R., Lamont, A., and Garland, P.B. 1980. The mechanism of proton translocation driven by the respiratory nitrate reductase complex of *Escherichia coli*. *Biochem. J*. 190: 79-94.
- Krishtalik, L.I., Tae, G.S., Cherepanov, D.A., and Cramer, W.A. 1993. The redox properties of cytochromes *b* imposed by the membrane electrostatic environment. *Biophys. J*. 65: 184-95.
- Lancaster, C.R.D. 1998. Ubiquinone reduction and protonation in photosynthetic reaction centres from *Rhodospseudomonas viridis*: X-ray structures and their functional implications. *Biochim. Biophys. Acta*. 1365: 143-150.
- Lancaster, C.R.D., Kröger, A., Auer, M., and Michel, H. 1999. Structure of fumarate reductase from *Wolinella succinogenes* at 2.2Å resolution. *Nature*. 402: 377-385.
- Magalon, A. 1997. Etude du transfert d'électron au sein d'un complexe multimerique respiratoire de type molybdéozyme, la nitrate reductase A chez *Escherichia coli*. Université de la Méditerranée, Marseille, pp. 86-90.
- Magalon, A., Asso, M., Guigliarelli, B., Rothery, R.A., Bertrand, P., Giordano, G., and Blasco, F. 1998a. Molybdenum cofactor properties and [Fe-S] cluster coordination in *Escherichia coli* nitrate reductase A: investigation by site-directed mutagenesis of the conserved His-50 residue in the NarG subunit. *Biochemistry*. 37: 7363-7370.
- Magalon, A., Lemesle-Meunier, D., Rothery, R.A., Frixon, C., Weiner, J.H., and Blasco, F. 1997a. Heme axial ligation by the highly conserved His residues in helix II of cytochrome *b*_{Nr} of *Escherichia coli* nitrate reductase A (NarGHI). *J. Biol. Chem*. 272: 25652-25658.
- Magalon, A., Rothery, R.A., Giordano, G., Blasco, F., and Weiner, J.H. 1997b. Characterization by electron paramagnetic resonance of the role of the *Escherichia coli* nitrate reductase (NarGHI) iron-sulfur clusters in electron transfer to nitrate: an identification of a semiquinone radical intermediate. *J. Bacteriol*. 179: 5037-5045.
- Magalon, A., Rothery, R.A., Lemesle-Meunier, D., Frixon, C., Weiner, J.H., and Blasco, F. 1998b. Inhibitor binding within the NarL subunit (cytochrome *b*_{Nr}) of *Escherichia coli* nitrate reductase A. *J. Biol. Chem*. 273: 10851-10856.
- Moreno-Vivián, C., Cabello, P., Martínez-Luque, M., Blasco, R., and Castillo, F. 1999. Prokaryotic nitrate reduction: molecular properties and functional distinction among bacterial nitrate reductases. *J. Bacteriol*. 181: 6573-6584.
- Morpeth, F.F., and Boxer, D.H. 1985. Kinetic analysis of respiratory nitrate reductase from *Escherichia coli* K12. *Biochemistry*. 24: 40-46.
- Murray, L., Pires, R.H., Hastings, S.F., and Inglede, W.J. 1999. Models for structure and function in quinone binding sites: the *Escherichia coli* quinol oxidase, cytochrome *bo*₃. *Biochem. Soc. Trans*. 27: 581-585.
- Ohnishi, T., Moser, C.C., Page, C.C., Dutton, P.L., and Yano, T. 2000. Simple redox-linked proton-transfer design: new insights from structures of quinol-fumarate reductase. *Structure*. 8: R23-R32.
- Okun, J.G., Lümmen, P., and Brandt, U. 1999. Three classes of inhibitors share a common binding domain in mitochondrial complex I (NADH:ubiquinone oxidoreductase). *J. Biol. Chem*. 274: 2626-2630.
- Page, C.C., Moser, C.C., Chen, X., and Dutton, P.L. 1999. Natural

- engineering principles of electron tunnelling in biological oxidation-reduction. *Nature*. 402: 47-52.
- Philippot, L., and Højberg, O. 1999. Dissimilatory nitrate reductases in bacteria. *Biochim. Biophys. Acta*. 1446: 1-23.
- Potter, L.C., Millington, P., Griffiths, L., Thomas, G.H., and Cole, J.A. 1999. Competition between *Escherichia coli* strains expressing a periplasmic or a membrane-bound nitrate reductase: does Nap confer a selective advantage during nitrate-limited growth? *Biochem. J.* 344: 77-84.
- Potter, L.C., Millington, P.D., Thomas, G.H., Rothery, R.A., Giordano, G., and Cole, J.A. 2000. Novel growth characteristics and high rates of nitrate reduction of an *Escherichia coli* strain, LCB2048, that expresses only a periplasmic nitrate reductase. *FEMS Micro. Lett.* 185: 51-57.
- Richardson, D.J., and Watmough, N.J. 1999. Inorganic nitrogen metabolism in bacteria. *Curr. Opin. Chem. Biol.* 3: 207-219.
- Rothery, R.A., Blasco, F., Magalon, A., Asso, M., and Weiner, J.H. 1999a. The hemes of *Escherichia coli* nitrate reductase A (NarGHI): potentiometric effects of inhibitor binding to NarI. *Biochemistry*. 38: 12747-12757.
- Rothery, R.A., Chatterjee, I., Kiema, G., McDermott, M.T., and Weiner, J.H. 1998a. Hydroxylated naphthoquinones as substrates for *Escherichia coli* anaerobic reductases. *Biochem. J.* 332: 35-41.
- Rothery, R.A., Magalon, A., Giordano, G., Guigliarelli, B., Blasco, F., and Weiner, J.H. 1998b. The molybdenum cofactor of *Escherichia coli* nitrate reductase A (NarGHI): effect of a *mobAB* mutation and interactions with [Fe-S] clusters. *J. Biol. Chem.* 273: 7462-7469.
- Rothery, R.A., Trieber, C.A., and Weiner, J.H. 1999b. Interactions between the Molybdenum Cofactor and Iron-Sulfur Clusters of *Escherichia coli* Dimethylsulfoxide Reductase. *J. Biol. Chem.* 274: 13002-13009.
- Rothery, R.A., and Weiner, J.H. 1991. Alteration of the iron-sulfur composition of *Escherichia coli* dimethyl sulfoxide reductase by site-directed mutagenesis. *Biochemistry*. 30: 8296-8305.
- Rothery, R.A., and Weiner, J.H. 1993. Topological characterization of *Escherichia coli* DMSO reductase by electron paramagnetic resonance spectroscopy of an engineered [3Fe-4S] cluster. *Biochemistry*. 32: 5855-5861.
- Rothery, R.A., and Weiner, J.H. 1996. Interaction of an engineered [3Fe-4S] cluster with a menaquinol binding site of *Escherichia coli* DMSO reductase. *Biochemistry*. 35: 3247-3257.
- Rothery, R.A., and Weiner, J.H. 1998. Interaction of a menaquinol binding site with the [3Fe-4S] cluster of *Escherichia coli* fumarate reductase. *Eur. J. Biochem.* 254: 588-595.
- Salerno, J.C. 1984. Cytochrome electron spin resonance lineshapes, ligand fields, and components stoichiometry in ubiquinol-cytochrome *c* oxidoreductase. *J. Biol. Chem.* 259: 2331-2336.
- Saribas, A.S., Ding, H., Dutton, P.L., and Daldal, F. 1997. Substitutions at position 146 of cytochrome *b* affect drastically the properties of heme b_L and the Q_o site of *Rhodobacter capsulatus* cytochrome bc_1 complex. *Biochim. Biophys. Acta*. 1319: 99-108.
- Sato-Watanabe, M., Itoh, S., Mogi, T., Matsuura, K., Miyoshi, H., and Anraku, Y. 1995. Stabilization of a semiquinone radical at the high-affinity quinone-binding site (Q_H) of the *Escherichia coli* *bo*-type ubiquinol oxidase. *FEBS Lett.* 374: 265-269.
- Sato-Watanabe, M., Mogi, T., Ogura, T., Kitagawa, T., Myoshi, H., Iwamura, H., and Anraku, Y. 1994. Identification of a novel quinone-binding site in the cytochrome *bo* complex from *Escherichia coli*. *J. Biol. Chem.* 269: 28908-28912.
- Smirnova, I.A., Hägerhäll, C., Konstantinov, A.A., and Hederstedt, L. 1995. HOQNO interaction with cytochrome *b* in succinate:menaquinone oxidoreductase from *Bacillus subtilis*. *FEBS Lett.* 359: 23-26.
- Thompson, J.D., Higgins, D.G., and Gibson, T.J. 1994. CLUSTAL W: improving the sensitivity of progressive multiple sequence alignment through sequence weighting, positions-specific gap penalties and weight matrix choice. *Nucleic Acids Res.* 22: 4673-4680.
- Trieber, C.A., Rothery, R.A., and Weiner, J.H. 1996. Engineering a novel iron-sulfur cluster into the catalytic subunit of *Escherichia coli* dimethylsulfoxide reductase. *J. Biol. Chem.* 271: 4620-4626.
- Valkova-Valchanova, M.B., Saribas, A.S., Gibney, B.R., Dutton, P.L., and Daldal, F. 1998. Isolation and characterization of a two-subunit cytochrome bc_1 subcomplex from *Rhodobacter capsulatus* and reconstitution of its bihydroquinone oxidation site (Q_o) site with purified Fe-S protein subunit. *Biochemistry*. 37: 16242-16251.
- van Ark, G., and Berden, J.A. 1977. Binding of HQNO to beef-heart submitochondrial particles. *Biochim. Biophys. Acta*. 459: 119-137.
- Vincent, S.P., and Bray, R.C. 1978. Electron paramagnetic resonance studies on nitrate reductase from *Escherichia coli* K12. *Biochem. J.* 171: 639-647.
- von Heijne, G. 1989. Control of topology and mode of assembly of a polytopic membrane protein by positively charged residues. *Nature*. 341: 456-458.
- Walker, F.A., Huynh, B.H., Scheidt, W.R., and Osvath, S.R. 1986. Models of the cytochromes *b*. Effect of axial ligand plane orientation on the EPR and Mössbauer spectra of low spin ferrihemes. *J. Am. Chem. Soc.* 108: 5288-5296.
- Wallace, B.J., and Young, I.G. 1977. Role of quinones in electron transport to oxygen and nitrate in *Escherichia coli*. Studies with a *ubr men* double quinone mutant. *Biochim. Biophys. Acta*. 461: 84-100.
- Westenberg, D.J., Gunsalus, R.P., Ackrell, B.A.C., Sices, H., and Cecchini, G. 1993. *Escherichia coli* fumarate reductase *frdC* and *frdD* mutants. Identification of amino acid residues involved in catalytic activity with quinones. *J. Biol. Chem.* 268: 815-822.
- Xia, D., Yu, C., Kim, H., Xia, J., Kachurin, A.M., Zhang, L., Yu, L., and Deisenhofer, J. 1997. Crystal structure of the cytochrome bc_1 complex from bovine heart mitochondria. *Science*. 277: 60-66.
- Yang, X., Yu, L., and Yu, C.A. 1997. Resolution and reconstitution of succinate-ubiquinone reductase from *Escherichia coli*. *J. Biol. Chem.* 272: 9683-9689.
- Yu, L., Xu, J., Haley, P.E., and Yu, C. 1987. Properties of bovine heart mitochondrial cytochrome b_{560} . *J. Biol. Chem.* 262: 1137-1143.
- Yun, C., Crofts, A.R., and Gennis, R.B. 1991. Assignment of the histidine axial ligands to the cytochrome b_H and cytochrome b_L components of the bc_1 complex from *Rhodobacter sphaeroides* by site-directed mutagenesis. *Biochemistry*. 30: 6747-6754.
- Zhang, Z., Huang, L., Shulmeister, V., Chi, Y., Kim, K.K., Hung, L., Crofts, A.R., Berry, E.A., and Kim, S. 1998. Electron transfer by domain movement in cytochrome bc_1 . *Nature*. 392: 677-684.

